International Journal of Nanoelectronics and Materials
Volume 15 (Special Issue) December 2022 [183-192]

Endless Coreless Fiber Sensor Coated with Gold and Graphene for Respiratory Monitoring System

Haneen D. Abdulkareem[1], Ali A. Alwahib[1,*], and Bushara R. Mahdi[2]

[1]Laser and Optoelectronics Department, University of Technology-Iraq, Baghdad, Iraq
[2]Ministry of Science and Technology, Material Researcher Department, Laser and Optoelectronics Center, Iraq-Baghdad

ABSTRACT

Traditional methods are used to measure respiratory rates. These methods rely on the number of times the chest inflates and contracts. Other methods may be inaccurate or take time. So, based on past and recent research, the optical sensor method is very efficient and real-time sensing. This type of sensor is always the most demanded in current and future research so, we proposed a respiratory monitoring system based on an optical fiber sensor. The sensor consists of coreless fiber spliced with multimode fiber on one side coated with nanogold particles and graphene. The sensitivity and response time of the sensor were calculated with coated gold and with coated with gold & graphene; when coated with gold were 473.2 pm/%RH and 2.3 sec respectively, and when coated with gold & graphene was 513.8 pm/%RH and 1.5 sec respectively. The result showed that when breathing increased, the intensity of light decreased. The sleeping case of breathing has more intensity value than the intensity of working sport value.

Keywords: Coreless fiber, gold, graphene, sensor, respiratory rate

1. INTRODUCTION

Respiratory factors instance of respiratory rate (a respiratory volume and gas reciprocity can be obtained employment the humidity, temperature difference, and carbon dioxide (CO_2) of the flow of the air). Also, it is probably to control respiratory functions through calculating thoracic and abdominal variations [1].

The respiratory rate can be defined as the number of breaths inhaled and exhaled that a person takes in 60 seconds. This rate is measured when the person is entirely at rest in a chair and includes the number of breaths for a minute by counting the chest rises [2]. It is also important to mention that the regular respiratory rate changes because of many health factors, such as age, gender, and in case of illness, high body temperature, and other medical conditions, the respiratory rate changes and is higher than the average rate [3][4][5].

These parameters often indicate the patient's psychological and physical condition, and permanent monitoring is important to measure necessary patient factors in patients or high-risk bearings [1]. The function of the respiratory system is based on electrical sensors, i.e., using a capacitive sensor, pressure sensor, and pyroelectric sensor, others use an optical-based sensor using optical fiber. Selectivity, sensitivity, lightweight, smaller size, accuracy, flexibility, and reversibility made the form of fiber optic is the best tool for multifunction sensors. This optical tool can be used in diverse mensuration in different areas [6]. Many calculations can be done in using optical fiber such as in field of refractive index (RI) [7], vibration [8], rotation [9], temperature [10], magnetic fields [11], pressure [12], humidity [13], acceleration [14], etc. In the medical Optical fiber sensors become very requisite in civil modern life [15], [16], and defense

* Ali.A.Alwahib@uotechnology.edu.iq

applications [17]. Presently, fiber optic sensor are utilized to reveal distinct body and chemical factors of clinical avails.

M. Shao et al. [18] illustrated a test stickiness sensor based on photonic crystal fiber manufactured by sandwiching a decrease between photonic crystal fiber and a standard single mode fiber. The decrease and collapsed locale in photonic crystal fiber energize high-order modes and couple them with center mode to create a Michelson interferometer. J. Mathew et al. [19] designed a breathing detecting framework utilizing photonic crystal fiber sort LMA-10, outlined for unending single-mode fiber. F. c. Favero et al. [20] designed a respiratory checking sensor.

The interferometer was fabricated by splicing photonic cystal fiber with single mode fiber, but the photonic crystal fiber segment was ensured with a glass tube protected with another metallic tube. In this research we proposed an active sensor based on multimode fiber – coreless fiber coated with gold nanoparticles and graphene to produce a very sensitive sensor by using laser as a source in visible spectrum. Coated with nanogold & graphene to enhance the humidity absorpition thart obtained from the exhalation, because the ability of graphene to absorb moisture.

2. MATERIALS AND METHODS

The fabrication of the interferometer is easy and straightforward since it only includes cleaving and fusion splicing, which can be carried out with common fiber tools and equipment [21].

The conventional multimode fiber has been used with coreless fiber with 125 μm in diameter. A short section with coreless fiber length 5 cm using in this sensor, Spliced the coreless fiber with MMF from one side. The taper was fabricated through conventional fusion splicer, and then etching the fiber by inserted a droplet of hydrofluoric acid (HF) amongst the coreless fiber with 40% concentration. To produce an active sensor coated it firstly with gold nanoparticles, to generate surface Plasmon resonance (SPR). Surface plasmon resonance achieved and obtained wavelength shifting because the gold demonstrates a higher shift of resonance parameter to change in refractive index of sensing layer and is chemically stable. by using plasma sputtering coating process as shown in Figure 1, a target or a metal precursor, that desired to be deposited, is bombarded with energetic ions of inert gases (e.g., argon or helium). The forceful collision of these energetic ions with the target ejects target metal atoms into space. These metal atoms are then deposited on the substrate material forming a metallic film. The target is cooled by water so that little radiation heat is generated. We used 500 V power supply and 27 mA for current and $8*10^{-1}$ mbar for pressure with gold purity of 99.9% and thickness of 1mm in this process, and take the first results. Then coated the sensor with a graphene additional to nanogold particles with 20 nm thickness, because it's high ability to absorb moisture in the same way as coated gold, and also take the results.

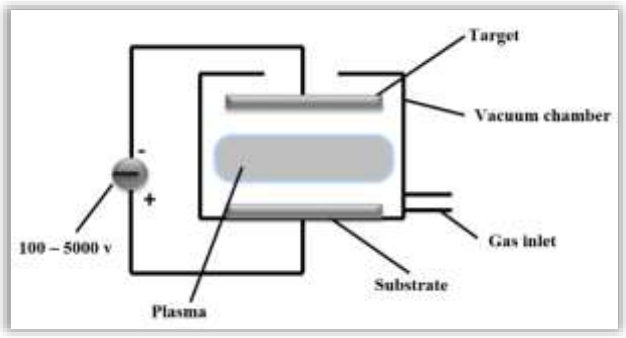

Figure 1. Schematic diagram of the mechanism of magnetron sputter coating machine.

After the all processes to fabricate the sensor were done, the setup of experiment is connected, the experimental setup is shown in Figure 2. 650 nm laser source connected with the fabrication sensor by the 3-dB fiber optical coupler 50/50. Fiber optic coupler divided the input signal into two parts: one went to the sensor, and the other went to the optical spectrometer (OSA- HR2000), when the spectrometer connected with PC to show the data results. When the signal reaches the sensing surface, this surface will act as a reflected mirror to the signal. The PC is the final destination of the reflected signal from the second arm of the optical coupler throughout the spectrometer. The process was repeated for each of the different breathing cases.

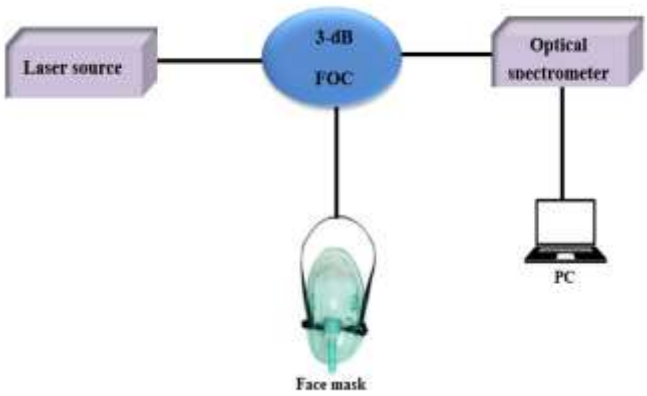

Figure 2. Experimental setup of proposed sensor.

The sensor was inserted into the oxygen mask pass and connected the sensor to the optical coupler. The oxygen mask was placed and tested on the person's face. The inhalation and exhalation were calculated at each breathing process and sensing the moisture associated with the inhalation and exhalation processes.

This sensor was first used on normal air and considered a reference; then, it was used on daily human activities, such as sitting, walking, jogging, exercising, and sleeping. The light intensity was calculated in each case using an optical spectrometer, and the transmittance and sensitivity were calculated.

3. RESULTS AND DISCUSSION

3.1 Coated with Nanogold Particles

Firstly, the sensor was tested by measuring different breathing states, and by connecting it to the spectrometer, the light intensity was calculated as a function of wavelength.

Figure 3 shows the transmission spectra of coreless fiber – MMF sensor for different breathing cases. From figure 3(a) and Table 1, the wavelength shift from 658.06 to 670.15 nm with increase in speed of breathing, because of the gold nanoparticles (Au NPs) possess distinct physical and chemical attributes that make them excellent scaffolds for the fabrication of novel chemical and biological sensors. When the breathing rate increases, the dielectric properties of the (Au NPs) change, resulting in a shift in the resonance wavelength [22]. So, the higher the intensity was at lower respiratory rate where the lower the intensity was at higher respiratory rate and the normal respiratory rate ranges between them. The intensity in all cases progressively increased until it reached the highest value at the wavelength of the red laser and then went back down. The intensity was 299.14 at 658.06 nm wavelength. Therefore, the highest intensity in the state of sleep, which is the lowest rate of respiration, where it is approximately ten breaths per minute. At the normal state of breathing (sitting), the intensity gradually decreased at each state of

breathing. The respiratory rate is approximately 14 breaths per minute. In the sitting state, the intensity was 284 at 661.64 nm wavelength; the respiratory rate increased because the walking state was close to the normal state. However, the intensity was 272.11 at 663.11 nm wavelength, close to the previous state.

In the two last cases, it was less intensity, because running and working sport increased the respiratory rate, which is approximately 30 or more, so, the intensity of light at running was 269 at 665.23 nm wavelength, where the intensity at working sport which is considered the least intensity and highest respiratory rate was 182.33 at 670.15 nm wavelength. As a results from all cases it had been observed red shift wavelength at the higher the respiratory rate and the lower the intensity. The figure of merit (FOM) is a significant parameter used to evaluate the performance of the SPR sensors. A large FOM indicates high detection accuracy. Additionally it helps to expand the detection limit. FOM can be evaluated as follows:

$$FOM\ (RH^{-1}) = S_W / FWHM \quad (1)$$

Where S_W is the wavelength sensitivity and FWHM defined as full width half maxima. FOM was calculated for each cases.

Transmittance (T) is the fraction of incident light which is transmitted. In other words, it's the amount of light that "successfully" passes through the substance and comes out the other side. So, to calculate transmittance we used this equation.

$$T = I_{out} / I_{in} \quad (2)$$

Where Iin is the intensity of incident light, and Iout is intensity of that light after it passed through the sample.

From Figure 3(b) and Table 2, used equation 2 to found the transmittance of the sensor, that when increased the respiratory rate the transmittance also increased and vice versa, and also shown the wavelength shifting. So, Figure 3.B shows the opposite of Figure 3(a) because the measured intensity is divided by the reference intensity. Therefore, working sport was the highest transmittance at value 0.3260 at 652.68 nm wavelength and less transmittance was at sleeping at value of 0.8346 at

652.44 nm wavelength between them the other cases from running to sitting with a value of 0.502 at 653.13 nm wavelength for running and 0.6274 at 651.34 nm wavelength for sitting and finally 0.562 at 652.24 nm wavelength for walking.

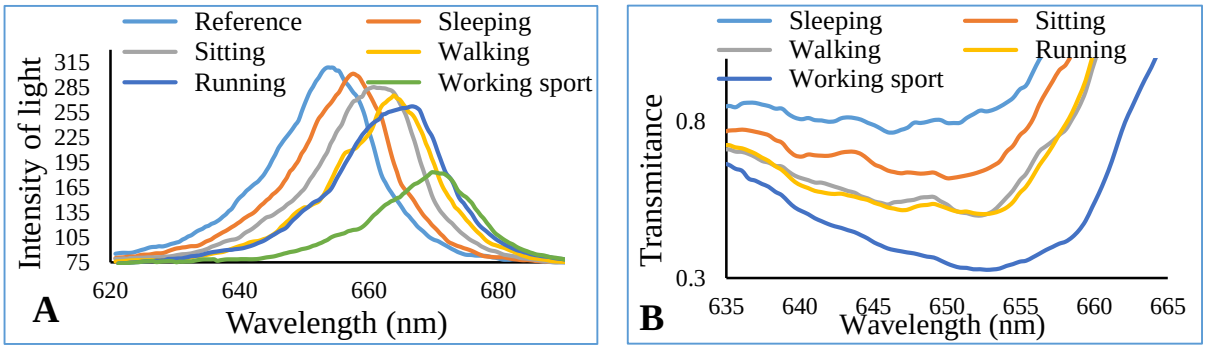

Figure 3. a) Transmission spectra of (coreless – SMF) sensor for different breathing cases b) transmittance of the sensor with nanogold coating.

Table 1 Numerical results for proposed sensor

Breathing Cases	Intensity of Light	Shifting Wavelength	Figure of Merit (FOM)
Sleeping	299.14	658.06	0.021
Sitting	284	661.64	0.022
Walking	272.11	663.44	0.023
Running	269	665.23	0.0215
Working sport	182.33	670.15	0.024

Table 2 Numerical transmittance results for proposed sensor

Breathing Cases	Transmittance	SPR Wavelength
Working sport	0.3260	652.68
Running	0.502	653.13
Walking	0.562	652.24
Sitting	0.6274	651.34
Sleeping	0.8346	652.44

Figure 4 shows the relation between relative humidity and shifting wavelength of this sensor. By fabricating the breathing sensor based on humidity absorption and by calculating the shifting wavelength introduced from the sensing respiratory rate. So, Figure 4 shows the relation between shifting wavelength and change in relative humidity, by taking the slope of the curve we calculated the sensitivity of the sensor that was 473.2 pm /% RH. Response time of this sensor was 2.3 sec.

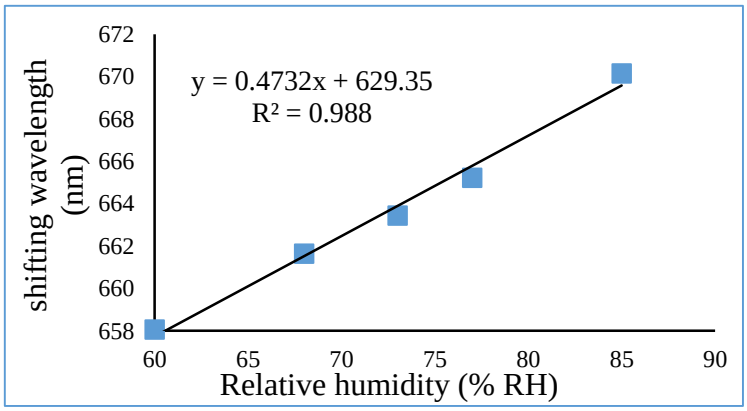

Figure 4. Relation between relative humidity and shifting wavelength for nanogold coating sensor.

3.2 Coated with Gold and Graphene

Figure 5 shows the reference wave of the sensor when coated with gold and coated gold & graphene, when compared the results found the gold & graphene coated was less intensity than just gold because graphene increased the absorbition of the sensor so the intensity decreased.

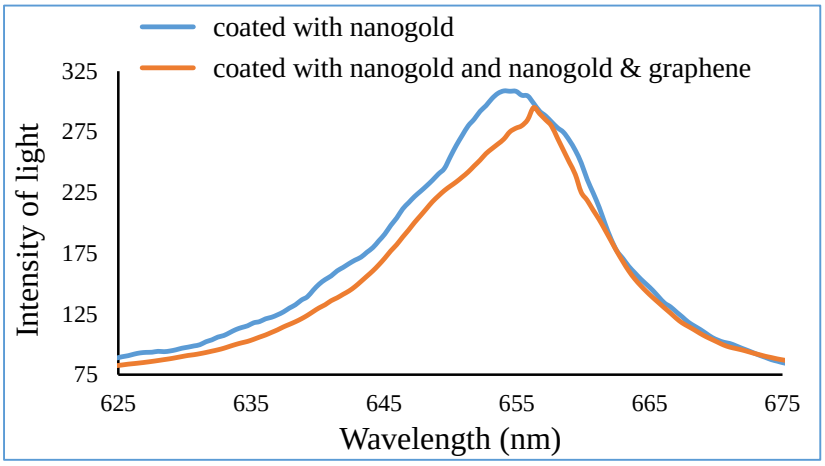

Figure 5. Reference wave for gold and gold & graphene coated.

Figure 6(a) shows the different cases of respiration, when taking the sleeping case the intensity was 98 at 667.02 nm wavelength, and for sitting was 95.62 at 669.25 nm wavelength, and for walking and runing 94.49 at 672.38 nm wavelength 89.7 at 674.62 nm wavelength respctively, and finaly for working sport was 86 at 677.3 nm wavelength. FOM also showed in Table 3.

Figure 6(b) shows the transmittance spectra of sensor when coated with gold & graphene, when taking working sport breathing case the transmission was 0.4326 at 656.27 wavelength and for running was 0.5518 at 653.13 nm wavelength and for walking and sitting were 0.6743 and 0.7303 at 653.58 nm and 651.34 nm wavelength respectively and finally for sleeping was 0.8181 at 648.65 nm wavelength.

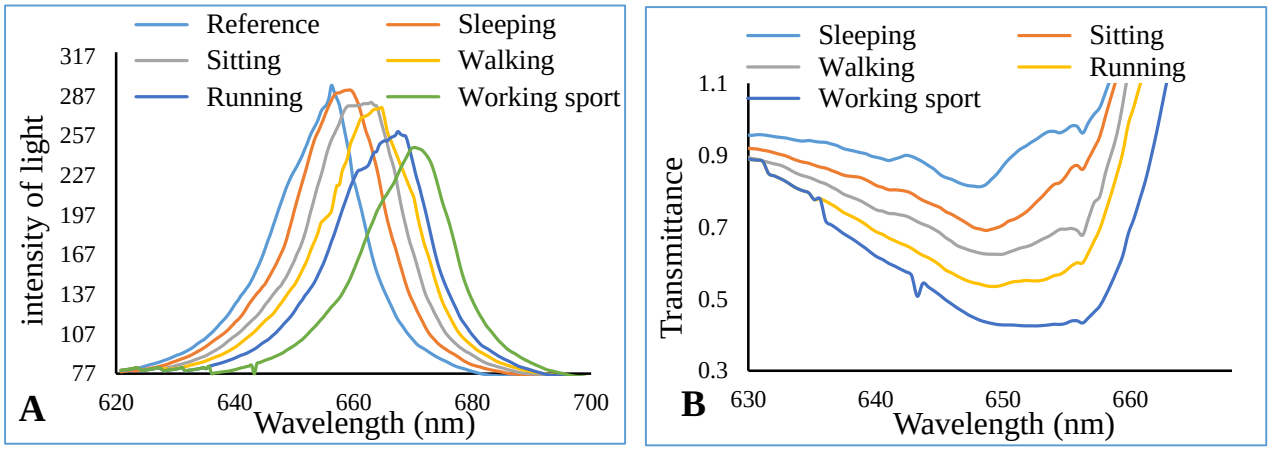

Figure 6. a) Transmission spectra of coreless fiber interferometer coated with gold & graphene
b) Transmittance spectra of proposed sensor.

Table 3. Numerical intensity results of the proposed sensor

Breathing Cases	Intensity of Light	Shifting Wavelength	Figure of Merit (FOM)
Sleeping	290.04	659.85	0.022
Sitting	276	663.44	0.0224
Walking	278	664.77	0.0220
Running	258	667.91	0.024
Working sport	246	670.59	0.026

Table 4. Numerical transmittance results for proposed sensor

Breathing Cases	Transmittance	SPR Wavelength
Working sport	0.4326	656.27
Running	0.5518	653.13
Walking	0.6743	653.58
Sitting	0.7303	651.34
Sleeping	0.8181	648.65

Figure 7 shows the relation between shifting wavelength and change in relative humidity, by taking the slope of the curve we calculated the sensitivity of the sensor that was 513.8 pm / %RH. The response time of this sensor was 1.5 sec.

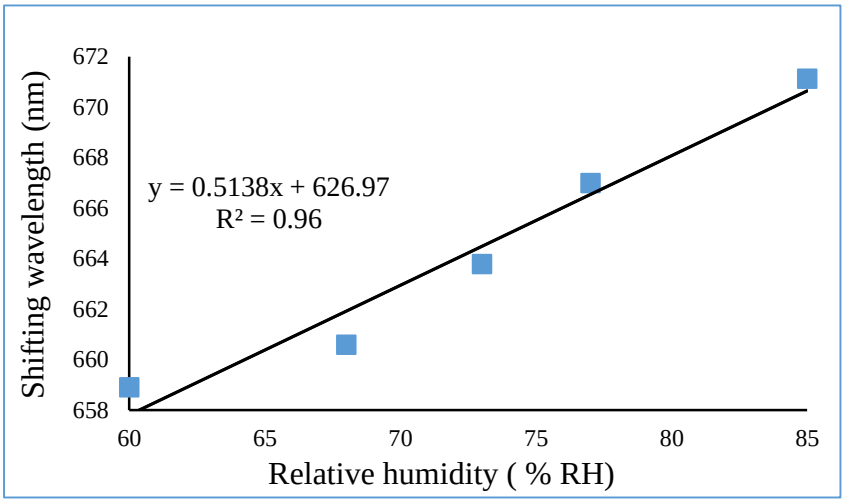

Figure 7. The relation between wavelength and relative humidity for the breathing sensor coated with gold & graphene.

4. COMPRESSION OF TWO SENSORS

From Table 6 and Figure 8, obvious the difference results for the sensor when coated with gold and gold & graphene, it appear that when coated just nanogold the sensitivity is less than that coated with nanogold & graphene and the shifting wavelength increased because graphene is used to improve the performance of sensor due to the ability of graphene to absorb moisture from air because it composed of carbon and hydrogen.

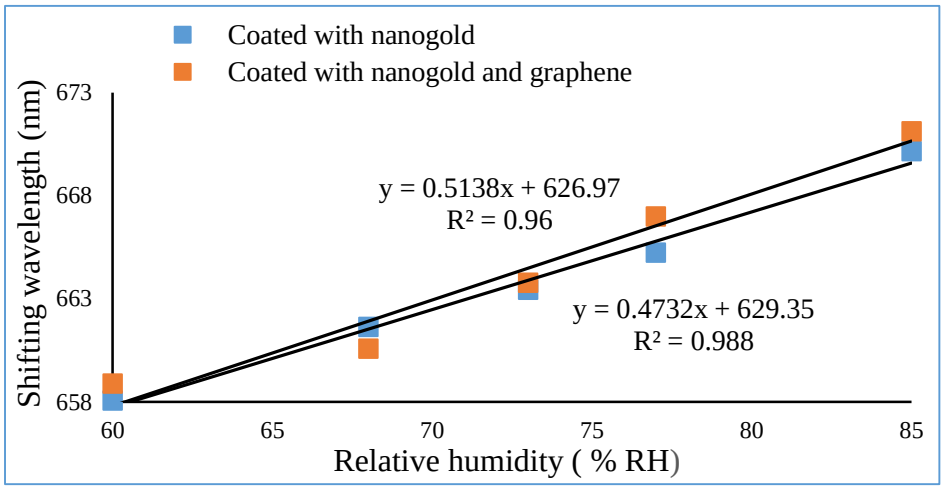

Figure 8. Wavelength shifts vs relative humidity of sensor coated with nanogold and nanogold & graphene.

Table 6. Comparison in parameter of two sensors

Breathing case	Coated gold			Coated gold & graphene		
	Intensity	Shifting	FOM	Intensity	Shifting	FOM
Sleeping	299.14	4.03	0.021	290.04	3.58	0.022
Sitting	284	3.58	0.022	276	3.59	0.0224
Walking	272.11	1.8	0.023	270	1.33	0.0220
Running	269	1.79	0.0215	258	3.14	0.024
Working sport	182.33	4.92	0.024	246	2.68	0.026
Sensitivity	473.2 pm /% RH			513.8 pm / %RH		
Response time	2.3 sec			1.5 sec		
Resolution	0.105 RH			0.097 RH		
Detection limit	2.218 pm			1.887 pm		

5. CONCLUSION

A successful respiratory monitoring system based on a coreless fiber interferometer coating with nanogold particles and gold & graphene has been developed. The system was able to monitor respiratory rates for various activities based on calculating light intensity. When the respiratory rate increased, the light intensity decreased and made shifting wavelength for each activity. The highest intensity in the state of sleep is the lowest rate of respiration, in the sitting and walking states the intensity decreased because the respiratory rate increased in those cases and last states (running and working sport) were less intensity. The transmittance of this sensor was also measured.

REFERENCES

[1] W. J. Yoo et al., Development of optical fiber-based respiration sensor for noninvasive respiratory monitoring, Opt. Rev., vol. 18, no. 1, (2011), pp. 132–138.
[2] C. DA Charlton P, Birrenkott DA, Bonnici T, Pimentel MA, Johnson AE, Alastruey J, Tarassenko L, Watkinson PJ, Beale R, Breathing Rate Estimation from the Electrocardiogram and Photoplethysmogram: a review, Biomed. Eng. (NY)., vol. 11, (2018), pp. 2–20.
[3] L. P. Bailón R, Sõrnmo L, Advanced Methods and Tools for ECG Data Analysis - ECG Derived Respiratory Frequecy estimation, (2016).
[4] M. Y. M. Noor, G. Rajan, and G. D. Peng, Microstructured fiber sealed-void interferometric humidity sensor, IEEE Sens. J., vol. 14, no. 4, (2014), pp. 1154–115.
[5] G. O. Y. T. L. Yeo, T. Sun, K. T. V. Grattan, Fibre-optic sensor technologies for humidity and moisture measurement, Sens. Actuators A, Phys., vol. 144, no. 2, (2008), pp. 280–295.
[6] A. Arifin, N. Agustina, S. Dewang, I. Idris, and D. Tahir, Polymer Optical Fiber-Based Respiratory Sensors: Various Designs and Implementations, J. Sensors, vol. (2019), pp. 7–12.
[7] T.-H. Xia, A. P. Zhang, and B. G. and J.-J. Zhu, Fiber optic refractive-index sensors based on transmissive and reflective thin-core fiber modal interferometers, Opt. Commun., vol. 283, no. 10, (2010).
[8] J. M. C. Yoany Rodríguez García and J. Goicoechea, Vibration Detection Using Optical Fiber Sensors, J. Sensors. Artic., (2010).
[9] W. C. Goss, R. Goldstein, M. D. Nelson, H. T. Fearnehaugh, and O. G. Ramer, Fiber-optic rotation sensor technology, Appl. Opt., vol. 19, (1980), pp. 852–858.
[10] H. J. Patrick, G. M. Williams, Kersey, A. D., J. R. Pedrazzani, and A. M. Vengsarkar, Hybrid fiber Bragg grating/long period fiber grating sensor for strain/temperature discrimination, IEEE Photonics Technol. Lett., vol. 8, (1980), pp. 1223–1225.
[11] M. Yang, J. Dai, C. Zhou, and D. Jiang, Optical fiber magnetic field sensors with TbDyFe magnetostrictive thin films as sensing materials, Opt. Express, vol. 17, no. 23, (2009), pp. 20777–20782.
[12] W. Wang, N. Wu, Y. Tian, and X. W. Christopher Niezrecki, Miniature all-silica optical fiber pressure sensor with an ultrathin uniform diaphragm, Opt. Express, vol. 18, no. 9, (2010), pp. 9006–9014.
[13] L. Xu, J. C. Fanguy, K. Soni, and S. Tao, Optical fiber humidity sensor based on evanescent-wave scattering, Opt. Lett., vol. 29, no. 11, (2004), pp. 1191–1193.
[14] S. Tai, K. Kyuma, and M. Nunoshita, Fiber-optic acceleration sensor based on the photoelastic effect, Appl. Opt., vol. 22, no. 11, (1982), pp. 1771–1774.
[15] S. C. Huang, W. W. Lin, M. T. Tsai, and M. H. Chen, Fiber optic in-line distributed sensor detection and localization of the pipeline leaks, Sensors Actuators A, vol. 135, (2007), pp. 570–579.
[16] L. Zou and O. M. Sezerman, Method and system for simultaneous measurement of strain and temperature, United States Pat., vol. 599, (2009).
[17] T. Kumagai, H. Soekawa, T. Yuhara, and H. Kajioka, Fiber optic gyroscopes for vehicle navigation systems, in Proceedings of SPIE, (1994), pp. 181–191.
[18] M. Shao, H. Sun, J. Liang, L. Han, and D. Feng, In-Fiber Michelson Interferometer in Photonic Crystal Fiber for Humidity Measurement, IEEE Sens. J., vol. 21, no. 2, (2021), pp. 1561–1567.
[19] J. Ma, H. H. Yu, X. Jiang, and D. S. Jiang, High-performance temperature sensing using a selectively filled solid-core photonic crystal fiber with a central air-bore, Opt. Express, vol. 25, no. 8, (2017), p. 9406.
[20] F. C. Favero, J. Villatoro, and V. Pruneri, Microstructured optical fiber interferometric breathing sensor, J. Biomed. Opt., vol. 17, no. 3, (2012), p. 037006.,
[21] and S. K. S. Zheng, Y. Zhu, Fiber humidity sensors with high sensitivity and selectivity based on interior nanofilm-coated photonic crystal fiber long period gratings, Sens.

Actuators B, vol. 176, (2013), pp. 264–274.
[22] H. S. Ali and M. A. Fakhri, An overview of Au & photonic crystal fiber of sensors, Mater. Sci. Forum, vol. 1002, no. Figure 1, (2020), pp. 282–289.